J. Fluid Mech. (1987), *vol.* 182, *pp.* 525–541
Printed in Great Britain

The formation of a layered structure when a stable salinity gradient is heated from below

By HARINDRA J. S. FERNANDO
Department of Mechanical and Aerospace Engineering, Arizona State University, Tempe, AZ 85287, USA

(Received 9 July 1986 and in revised form 12 February 1987)

It is well known that heating a stable salinity gradient from below leads to the formation of a series of turbulently convecting layers separated by stable diffusive interfaces. It is argued theoretically and demonstrated experimentally that the first mixed layer grows to a critical height δ_c, which is determined by a balance between the vertical kinetic and potential energies of the turbulent eddies, before a growing second layer separated from the first layer by a quasi-stationary stable density interface can be formed. Although the thermal boundary layer that develops over the propagating turbulent front can become unstable and form a second mixed region before the first layer grows to δ_c, the density interface formed between these two layers is not sufficiently stable to resist quick entrainment of the second layer into the lower layer. Some aspects of the growth of the first turbulent layer and possible application of the results to oceanic situations are also discussed.

1. Introduction

Studies on the formation and evolution of the oceanic microstructure are important in many areas of physical oceanography, in particular large-scale oceanic-circulation research. In a general sense, the microstructure is characterized by homogeneous turbulent layers separated by thin stable density interfaces. The vertical heat and salt transport through these stable layers plays a prominent role in determining the heat and salt budgets of the ocean. The early work on oceanic microstructure was mainly performed by skin divers (Linbaugh & Rechnitzer 1955; Woods 1968) and their qualitative observations, as well as subsequent quantitative studies (Thorpe 1977), have revealed that Kelvin–Helmholtz-type instabilities induced by drift shear and internal-wave shear are responsible for the formation of the microstructure patches. However, recent observations made with high-resolution instruments clearly demonstrate the possibility of other potential microstructure sources such as double-diffusive instabilities (Mack 1985) and near inertial-frequency shear (Gregg 1984). The importance of double diffusion in both small- and large-scale oceanic events is becoming widely accepted as a result of an increase in understanding of phenomena such as the role of salt fingering in determining the temperature–salinity relationship in mid-latitudes (Schmitt 1981) and the maintenance of the Marginal Ice Edge by the heat transport through a diffusive interface (Stegan, Hendricks & Muench 1985).

Turner & Stommel (1964) were the first to perform laboratory demonstrations on the formation of a series of convecting layers separated by thin stable density interfaces when a stably stratified fluid with respect to salt is heated from below.

Upon heating, a mixed layer, which was found to grow with time, appeared near the heating surface. Once it grew to a certain vertical size, a second layer, separated from the first layer by a stable density interface could be observed. This process continued, resulting in a series of convecting layers separated by density interfaces across which heat and salt transport occur due to molecular diffusion. Interestingly enough, similar layered structures have been observed in lakes and oceans where a bottom heat flux is associated with a stabilizing salinity gradient. Some pertinent examples are the regions of diffusion of warm salty waters of the Red Sea in the Gulf of Aden and in the Indian Ocean along the Somali Coast (Siedler 1968; Krause 1968), the spreading of Mediterranean water in the west central Atlantic (Siedler 1968), the near-bottom superadiabatic temperature gradients in deep parts of the Pacific Ocean (Lubimova *et al.* 1985), salt and temperature distribution in trenches containing hot brine in the central part of the Red Sea (Swallow & Crease 1965), Lake Kivu in East Africa (Newman 1976), and Lake Vanda in Antarctica (Hoare 1966; Shirtcliffe & Calhaem 1968).

Turner (1968) performed a quantitative study to estimate the thickness of the first convective layer at the instant of the formation of the second layer. This formulation has been extended by Huppert & Linden (1979) to predict the evolution of a series of layers. In this paper we report some further studies of this subject which were motivated by, and are based on, recent findings on the nature of turbulence and mixing in stably stratified fluids.

2. Theoretical considerations

2.1. *Turner's work*

With regard to the growth of the turbulent mixed layer, Turner (1968) suggested that mixing at the turbulent front occurs due to a Rayleigh–Taylor gravitational-overturning instability which results because of the destabilizing temperature gradient at the turbulent–non-turbulent boundary. Further, it was argued that the entrainment interface is marginally stable, thus maintaining the condition $\alpha\Delta T = \beta\Delta S$, where ΔT and ΔS are the temperature and salinity differences across the entrainment interface (figure 1), and α and β are the coefficients of thermal expansion and salinity contraction, respectively. If the heat flux supplied to the bottom layer is Q (equivalent to a buoyancy flux of $q_0 = \alpha g Q/\rho_0 C_p$, where ρ_0 is the reference density, C_p is the specific heat and g is the gravitational acceleration), then it is easily shown that the equations for heat and salt conservation are

$$\alpha g \Delta T = \frac{q_0 t}{h}, \tag{1a}$$

$$\beta g \Delta S = \tfrac{1}{2} N^2 h, \tag{1b}$$

where h is the mixed-layer depth, t is the time and N is the stability frequency (defined by $N^2 = -\beta g\,(\mathrm{d}S/\mathrm{d}z)_0$, with $(\mathrm{d}S/\mathrm{d}z)_0$ the salinity gradient). Hence, the time dependence of the mixed-layer depth can be written as

$$h = C q_0^{\frac{1}{2}} N^{-1} t^{\frac{1}{2}}, \tag{2}$$

where $C = \sqrt{2}$. In Turner's (1968) experiments, the values for C were found to vary between 1.06 and 1.63, with a mean of 1.30. The low value was attributed to the escape of heat from the top of the mixed layer that formed a thermal boundary layer

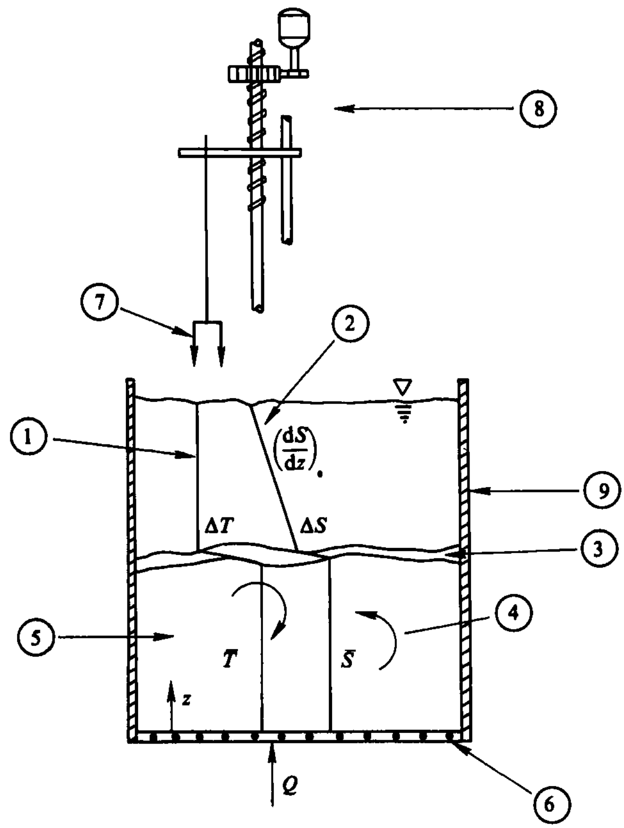

FIGURE 1. A schematic diagram of the experimental set-up. (1) Temperature distribution, (2) salinity distribution, (3) interfacial region, (4) rising thermal plumes, (5) mixed region, (6) array of heating elements, (7) conductivity and temperature probes, (8) traversing mechanism with position tracking, (9) insulated experimental tank.

above the advancing front. The analysis indicated that the thickness δ of this layer should take the form

$$\frac{\delta}{h} = 2\frac{k_{\mathrm{h}} N^2}{q_0}, \tag{3}$$

where k_{h} is the thermal conductivity. Turner (1968) proposed that a second mixed layer should appear on top of the growing first layer when the thermal boundary layer becomes unstable at a critical Rayleigh number $R_{\mathrm{c}} = \alpha g \Delta T \delta^3 / k_{\mathrm{h}} \nu$: or equivalently at a bottom mixed-layer height of

$$h_{\mathrm{c}} = (\tfrac{1}{4}R_{\mathrm{c}})^{\frac{1}{4}} \left(\frac{\nu q_0^3}{k_{\mathrm{h}}^2 N^8}\right)^{\frac{1}{4}}, \tag{4}$$

where ν is the kinematic viscosity. However, the value of R_{c} deduced from the experimental results ($\approx 2.4 \times 10^4$) was found to be an order of magnitude larger than the expected value ($\approx 10^3$) based on the extrapolation of the existing theory (Howard 1964; Veronis 1965; Currie 1967).

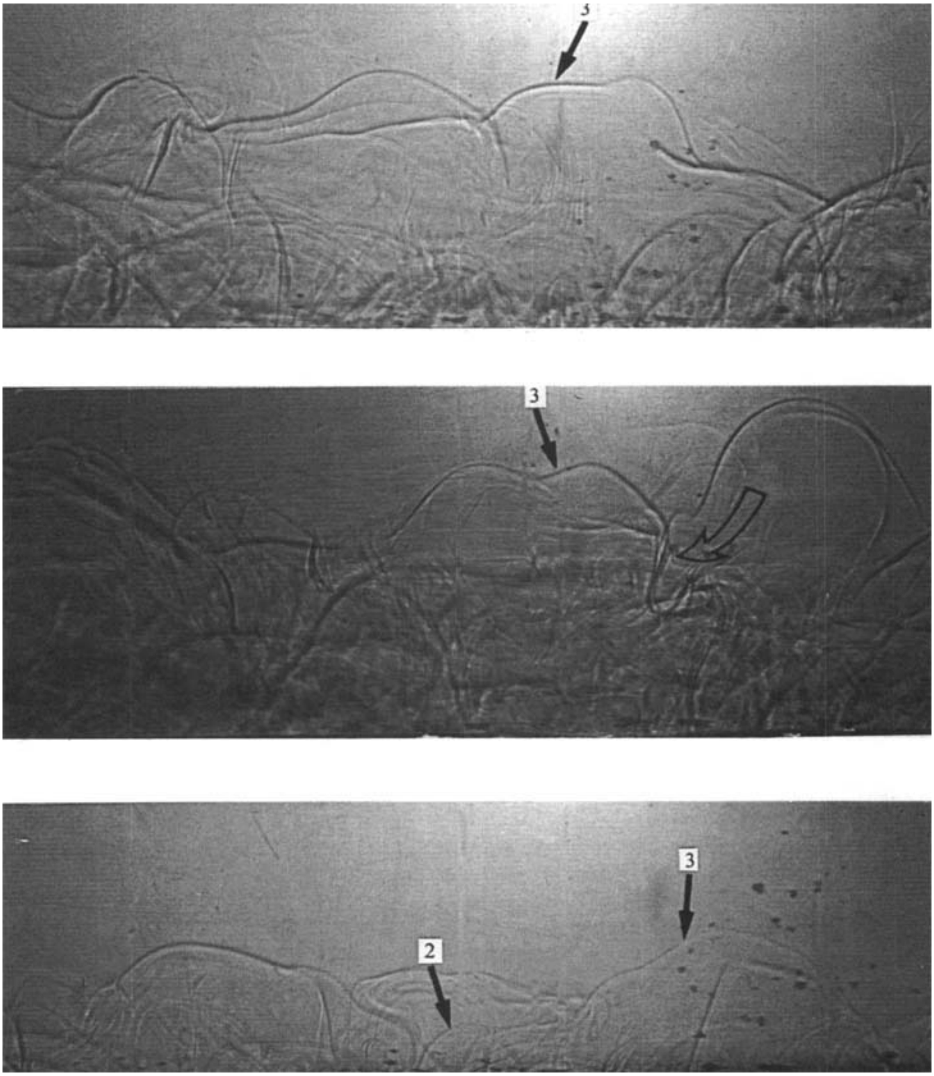

FIGURE 2. Initial growth of the mixed region – A close-up view. Notice the contorted nature of the interface (3) and sporadic ejection of fluid elements into the mixed-layer by the impinging eddies (4). The convection in the mixed region is driven by the 'thermals' or buoyant fluid elements (2) rising from the heated surface (1).

2.2. *Present work*

The present work was motivated by the belief that recent findings on the mechanics of stratified turbulent mixing can be used to gain a deeper insight into the layering process observed in salinity-stratified fluids subjected to bottom heating. It is useful to discuss some of these ideas that are particularly pertinent to the present investigation.

Careful observations of the entrainment process that occurs during the heating of a salinity gradient from below show that the entrainment is manifested by the engulfment of non-turbulent fluid by large-scale eddies near the interface (figure 2). The eddies impinging on the interface 'splash' the non-turbulent fluid into the mixed layer, thereby forming a highly contorted entrainment interface. This entrainment mechanism is quite similar to that observed by Deardorff, Willis & Stockton (1980), who studied convective mixing in heat-stratified fluids, and is rather different from what is expected if the Rayleigh–Taylor gravitational instability mechanism is responsible for mixing.

Recent experiments also indicate that there are at least two mixed-layer growth regimes. At very low Richardson number (or near the turbulent source), the large-scale mixed-layer eddies of the size of the integral lengthscale of turbulence have enough kinetic energy to entrain the non-turbulent fluid into the turbulent layer despite the buoyancy forces. Energetic eddies impinging on the interface distort it sufficiently that fine elements of the stratified fluid layer are drawn into turbulent regions and then homogenized with the rest of the fluid (Linden 1973). Under such conditions it is possible to estimate the entrainment rate by energy arguments, as most of the kinetic energy flux of the impinging eddies is used to entrain fluid from the non-turbulent layer. To this end, the entrainment hypothesis of Linden (1975), which states that the rate of change of potential energy due to mixing is proportional to the total kinetic energy flux available at the interface, is widely used. As the mixed layer grows, the integral lengthscale of the turbulence also increases and the effect of the buoyancy forces is increasingly felt. According to Fernando & Long (1983, 1985*a*, *b*) and Fernando (1987*a*), when the mixed layer grows to a critical height δ_c, where the vertical kinetic and potential energies of the eddies are of the same order,† the entrainment mechanism described above cannot take place and the density interface behaves more or less like a compliant wall to the mixed-layer turbulence. Now the large-scale, energy-containing eddies are not sufficiently energetic to perform turnover motions against the buoyancy forces and hence tend to flatten at the density interface, thus transferring the kinetic energy of their vertical velocity component to the horizontal components (Long 1978; Carruthers & Hunt 1986; Hannoun, Fernando & List 1987). Subsequent growth of the mixed layer beyond δ_c depends on the nature of the density interfacial layer that develops at the entrainment interface. Crapper & Linden (1974) have shown that the nature of the interfacial layer is dependent upon the Péclet number (based on the r.m.s. velocity and integral lengthscale near the interface) of the turbulence; at high Péclet numbers, the interfacial layer consists of sporadically breaking waves which contribute to the interfacial mixing, whereas, at low Péclet numbers, the interfacial layer tends to be purely diffusive (as in the present case) and the mixing rate is determined by the molecular diffusive flux across the interfacial layer. In both cases, the entrainment rate during subsequent growth is much smaller than the initial growth and hence, at the mixed-layer height δ_c, the density interface can be considered as quasi-stationary.

The above observations provide the basis for a new physical picture for the phenomena associated with heating a salinity gradient from below. The mixed layer initially grows by the action of large eddies until they are not energetic enough to do so. Hence, we may use Linden's entrainment hypothesis to calculate the initial entrainment rate. The rate of change of potential energy per unit area of the salt-stratified system due to mixing alone can be written as

$$\frac{\mathrm{d}\lambda}{\mathrm{d}t} = \tfrac{1}{4}\rho_0 N^2 h^2 \frac{\mathrm{d}h}{\mathrm{d}t}. \tag{5}$$

† This also implies a balance between the vertical inertia forces of the eddies and the opposing buoyancy forces against which the eddy turnover motions have to be performed.

If $(\mathrm{d}\lambda/\mathrm{d}t)$ is proportional to the kinetic energy flux available at the interface $\rho_0(\overline{w^2})^{\frac{3}{2}}$, where $(\overline{w^2})^{\frac{1}{2}}$ is the r.m.s. velocity near the interface, then

$$\tfrac{1}{4}N^2h^2\frac{\mathrm{d}h}{\mathrm{d}t} = \gamma(\overline{w^2})^{\frac{3}{2}}, \tag{6}$$

where γ is the 'mixing efficiency'†. If we use the usual parameterization for the r.m.s. velocity at a height h within a convective boundary layer (Hunt 1984), i.e.

$$(\overline{w^2})^{\frac{1}{2}} = C_1(q_0\,h)^{\frac{1}{3}}, \tag{7}$$

where henceforth C_1 will denote a constant, from (6) we obtain the same entrainment relation as Turner (1968), given by (2), with $C = (8\gamma C_1^3)^{\frac{1}{3}}$.

If this growth process continues until the kinetic and potential energy of the eddies are of the same order, then the limiting height of the mixed layer can be found from the equation (Long 1978)

$$\overline{w^2} = C_2\,\Delta b\delta_{\mathrm{c}}, \tag{8}$$

where Δb is the buoyancy jump across the interface, which is also the characteristic buoyancy variation of the eddies within the mixed layer. Using 1 (a, b), the expression for $\Delta b = g(\beta\Delta S - \alpha\Delta T)$ can be written in the form

$$\Delta b = C_3\,N^2h, \tag{9}$$

where $C_3 = (1/2 - C^{-2})$. From (7)–(9) we obtain

$$\delta_{\mathrm{c}} = C_4\left(\frac{q_0}{N^3}\right)^{\frac{1}{2}}, \tag{10}$$

where $C_4 = (C_1^2/C_2\,C_3)^{\frac{3}{4}}$. As discussed earlier, once the mixed layer grows to this thickness, its subsequent growth is negligibly slow. The interfacial region is diffusive and further mixing can occur only by molecular diffusion. Consequently, a thermal boundary layer can grow over the density interface; in turn, it becomes unstable and forms a second mixed layer.

Of course, in the above discussion we have neglected one important aspect of the problem, namely the possibility of the breakdown of the thermal boundary layer during the course of the initial growth. According to Turner (1968), this type of breakdown occurs when the thermal boundary layer above the advancing front grows to a thickness h_{c} given by (4), and hence

$$\frac{h_{\mathrm{c}}}{\delta_{\mathrm{c}}} = (\tfrac{1}{4}R_{\mathrm{c}})^{\frac{1}{4}}\frac{1}{C_4}\left[\frac{\nu q_0}{k_{\mathrm{h}}^2\,N^2}\right]^{\frac{1}{4}}. \tag{11}$$

Note that for laboratory‡ and oceanic situations¶ $h_{\mathrm{c}} \ll \delta_{\mathrm{c}}$ and hence one may expect a second mixed layer to form above the growing front. The initial thickness of the second layer is of the order of δ (given by (3)), and is small for the experiments of concern here. The question is whether such a two-layer system is sufficiently stable to permit the growth of a second layer above the first one.

† According to the measurements of Hannoun *et al.* (1987), for shear-free turbulent flows, the kinetic energy flux $\overline{q^2w}$, where $\overline{q^2}$ is the total kinetic energy, can be represented as $\overline{q^2w} \approx (\overline{w^2})^{\frac{3}{2}}$. Hence γ represents the fraction of total kinetic energy flux available at the interface expended for the production of potential energy.

‡ Typically $q_0 \approx 0.025$ cm²/s³ and $N \approx 1$ s⁻¹; hence using $R_{\mathrm{c}} \approx 10^3$ and $C_4 \approx 41.5$ (§4.3), we get $h_{\mathrm{c}}/\delta_{\mathrm{c}} \approx 0.35$.

¶ Typically $q_0 \approx 10^{-6}$ cm²/s³ and $N \approx 0.025$ s⁻¹; hence $h_{\mathrm{c}}/\delta_{\mathrm{c}} \approx 0.20$.

As discussed before, if h is less than δ_c, the turbulent eddies are energetic enough to cause entrainment by the engulfment mechanism described earlier and we might expect that the bottom mixed layer penetrates the second layer and engulfs it faster than the second layer can grow. (Note that due to the poor transport of heat across the interface, the convective activity in the second layer is low, as is the speed of propagation of its turbulent front.) In view of this argument, it is clear that a stable interface, which separates two convecting layers, can persist for extended time periods only when the lower layer grows to a thickness given by (10). Also the fact that $\delta_c \gg h_c$ may explain why Turner (1968) needed to choose a higher value of R_c to fit the layer-thickness data to (4).

3. Experimental procedure

The main objective of the experiments was to generate a series of convecting layers separated by diffusive interfaces under controlled laboratory conditions and to verify the validity of (10). The experiments were conducted in a tank 16 in. × 16 in. × 16 in. with sides of Plexiglas ($\frac{1}{2}$ in. thick). The sides are glued onto an aluminium base plate ($\frac{1}{4}$ in. thick) using superadhesive heat-resistant Loctite glue. The base plate was heated using heating tape (maximum power 2400 W) which was placed underneath the aluminium base in an array with equal spacings. An asbestos sheet ($\frac{1}{4}$ in. thick) was inserted between the coils and the base plate to ensure that the heat distribution was uniform. The sides of the tank, except for a window necessary for flow visualization, were insulated using Styrofoam sheets.

The linear salt stratification was obtained using the standard two-tank technique of Oster & Yamamoto (1963). The measurements of density ρ *vs.* depth z were made using two techniques, namely by measuring the electrical conductivity at various depths using a calibrated single-point conductivity probe and by measuring the salinity of fluid samples drawn from various depths using a temperature-compensated refractometer (AO Scientific Instruments Model no. 10419). The Brünt–Väisälä (stability) frequency N was calculated from a least-squares fit of the data using $N^2 = g(-\mathrm{d}\rho/\mathrm{d}z)/\rho_0$. Except near the bottom and top of the tank, an excellent linear stratification was obtained. Such behaviour was expected since, owing to zero-flux boundary conditions, the density gradient must adjust to zero at these two boundaries. The stability frequencies based on the two procedures agreed to within 5%.

The heating rate Q was controlled by a potentiometer, which was calibrated *a priori* for heat-flux/potentiometer-setting characteristics. The calibration was performed by measuring the temperature rise with time of a known mass m of fresh water contained in the experimental tank and using $Q = mC_a A^{-1}\,\mathrm{d}T/\mathrm{d}t$, where C_a is the specific heat evaluated at the average temperature of the calibration run, A is the cross-sectional area of the tank and T is the temperature. The thermodynamic data were extracted from Incropera & DeWitt (1985). It was found that the heat flux into the tank could be varied between 0.70 and 4.5 kW/m^2; the associated measurement uncertainties were estimated to be $\pm 5\%$.

The experiments were begun by setting the potentiometer to the desired value. The count of time was started when a thermocouple (Omega – fast response type) placed in the water, touching the aluminium base plate, showed a 2 °C increase. The growth of the turbulent layer with time was monitored with a shadowgraph. Because of the slight nonlinearity of the density gradient near the bottom, the measurements of mixed-layer depth were started when the mixed layer had grown to a thickness of about 2.2 cm. At a certain instant its growth virtually stopped and the formation of a second layer could be observed. At this point, the average depth of the lower layer δ_c was measured using two techniques: (*a*) by observing the average mixed-layer depth on a shadowgraph; and (*b*) by using conductivity/depth and temperature/depth profiles. In the latter case, the profiles were obtained by conductivity/temperature probes which were attached to a vertically traversing mechanism (figure 1). The position of the probe, electrical conductivity and the temperature were obtained in the form of a voltage output that could be recorded in analog form using (X, Y)-plotters and stored in a digital computer via a data acquisition system.

One of the concerns in the design of the experiment was the possibility of the formation of a horizontal layered structure due to the heating of the vertical walls (Chen, Briggs & Wirtz 1971). However, such a phenomenon could not be observed, perhaps due to the low thermal conductivity of the wall material.

4. Experimental results

4.1. *Visualization of the flow*

Once the heat is turned on, the thermal boundary layer that develops near the tank bottom becomes unstable and this leads to turbulent thermal convection. Shadowgraph observations reveal that the initial growth of the convective mixed layer is caused by the ejection of the non-turbulent fluid by the mixed-layer eddies (figures 2 and 3*a*–*c*), rather than being due to local instabilities at the entrainment interface. As the mixed layer grows a second mixed layer appears above the first one but, in a short time, the second layer is superseded by the advancing turbulent front of the first layer (figure 3*b*, *c*). Several similar appearance of the formation of a second layer and its entrainment into the growing lower layer were observed before the mixed-layer growth came to a virtual standstill at a particular height. The second mixed region that grew above the first layer was separated from the latter by a well-defined, quasi-stationary density interface (figure 3*d*). The second mixed region grew to a certain size and formed a second quasi-stationary interface above which a third mixed layer was found to develop (figure 3*e*). The process continued and formed a series of layers. The density interfaces between the convective layers remained stationary for some time and then started to migrate very slowly upwards, thus entraining fluid from the convecting layer above. Frequently an interface migrated and merged with the next one, but occasionally one broke up and the two surrounding layers mixed with each other vigorously. Observations made by injecting coloured dye into the bottom convecting layer revealed that initially the mass transfer rate across the interface is negligibly slow, but when the density difference across the interface falls below a certain value, the solute transfer rate increases substantially. By investigating the behaviour of a two-layer salt-stratified fluid

---

FIGURE 3. A sequence of photographs taken during the evolution of a series of layers. (*a*–*c*) represent the initial growth regime. The appearance of a second layer on top of the first layer can be clearly seen. The second layer formed during the initial growth is entrained into the faster growing lower layer until the mixed region grows to a thickness δ_c given by (10). (*d*) shows the diffusive interface formed at the mixed-layer height δ_c. Now the second mixed layer can grow without being entrained into the lower layer. Once it grows to a critical height a third layer is formed, as shown in (*e*). The symbols indicate (1) the advancing turbulent front, (2) the second layer formed owing to the breakdown of the thermal boundary layer, (3) engulfment of fluid into the lower layer, (4) the appearance of the first quasi-stationary density interface, (5) the second quasi-stationary density interface.

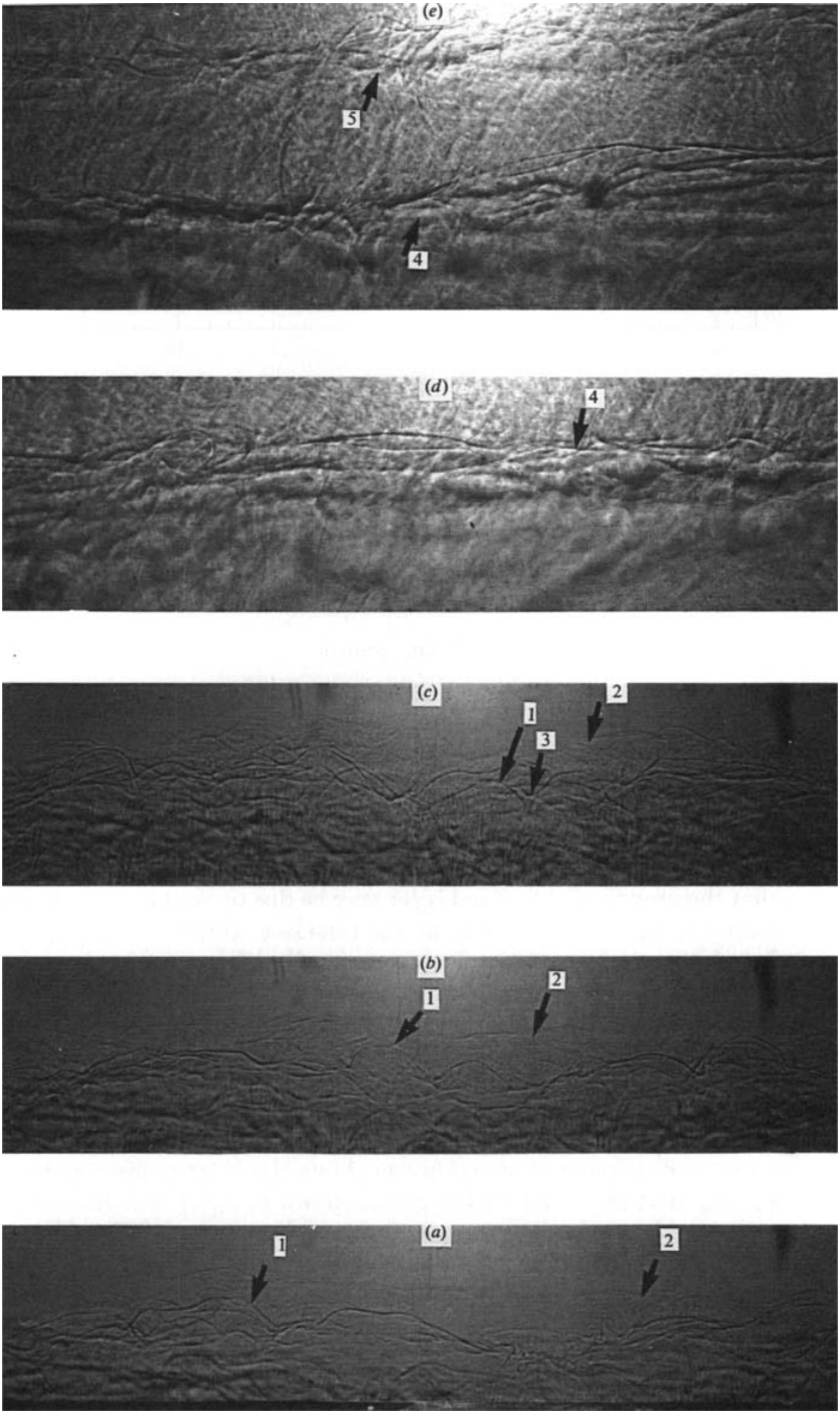

FIGURE 3. For caption see facing page.

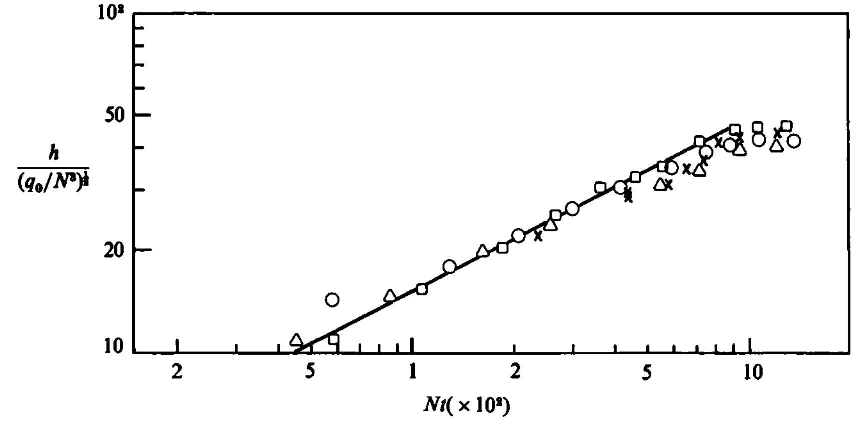

FIGURE 4. Variation of $h/(q_0/N^3)^{\frac{1}{2}}$ with Nt. The solid line represents the prediction (2) with $C = 1.5$. ○, $q_0 = 0.032\ \mathrm{cm^2/s^3}$, $N = 0.75\ \mathrm{s^{-1}}$; □, 0.02, 0.96; △, 0.032, 0.85; +, 0.02, 1.39.

subjected to a bottom heat flux, Fernando (1987*b*) has found that the interfacial movement occurs when the stability of the interface, or equivalently, a Richardson number based on the buoyancy jump across the interface, the depths of the convecting layers and the differential turbulence levels across it, falls below a critical value.

4.2. *Initial growth*

Figure 4 shows a plot of $h/(q_0/N^3)^{\frac{1}{2}}$ *vs.* Nt for several different experiments. A good agreement with the power law in (2) can be seen. The deviations at small Nt may reflect errors due to the use of an arbitrarily defined time origin in plotting the results. Note that the layer grows according to (2) and levels off at a lengthscale given by (10), with $h/(q_0 N^{-3})^{\frac{1}{2}} \approx 40$–$46$. The mean value of the constant C was found to be 1.50 with a standard error ± 0.075, compared with Turner's 1.26 ± 0.04, indicating an interfacial buoyancy jump $\Delta b = g(\beta \Delta S - \alpha \Delta T) = 0.13 g \alpha \Delta T > 0$. This result supports the notion that the growth of the mixed layer may be due to mechanical entrainment rather than the overturning instability at the interface. Hence $C = (8\gamma C_1^3)^{\frac{1}{2}} \approx 1.50$, and using $C_1 \approx 1.0$ we find $\gamma \approx 0.28$, which agrees well with $\gamma = 0.26$ values obtained in the previous mixing experiments of Narimousa & Fernando (1987).

Turner (1968) presents experimental results for h^2 *vs.* t, but does not provide data for times beyond the appearance of a second mixed layer. According to Huppert & Linden (1979), Turner (1968) has also observed the stoppage of the growth of the lower layer when a well-defined second layer is formed. Notice that the collapse of data at large h is not as good as that for intermediate values of h. This may be due to the formation and merging of mixed layers above the front as discussed in §2. It is also interesting that the shape of the graph shown in figure 4 is similar to that observed in the mechanical-mixing experiments of Fernando (1987*a*). The mixed layer initially grows rapidly due to the action of large eddies and then virtually stops when the vertical kinetic and potential energies are of the same order; a further slow growth is possible through the breaking of internal waves formed at the interface.

4.3. *Critical thickness of the lower layer*

In §2 it was argued that the thickness of the lower convecting layer that can remain quasi-stationary while sustaining an upper convecting layer should be given by (10). We have checked the validity of this theoretical result by measuring δ_c during

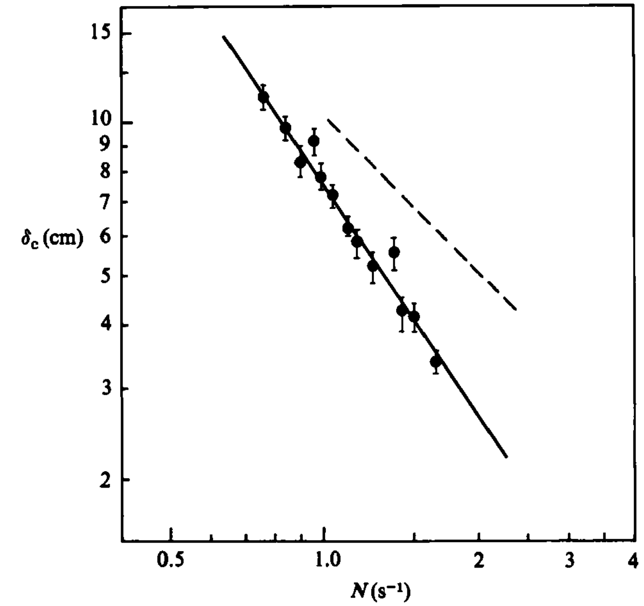

FIGURE 5. Variation of δ_c with N at constant $q_0 \simeq 0.032\ cm^2/s^3$. The solid line and broken lines indicate $-\frac{3}{2}$ and -2 slopes respectively corresponding to (10) and (4).

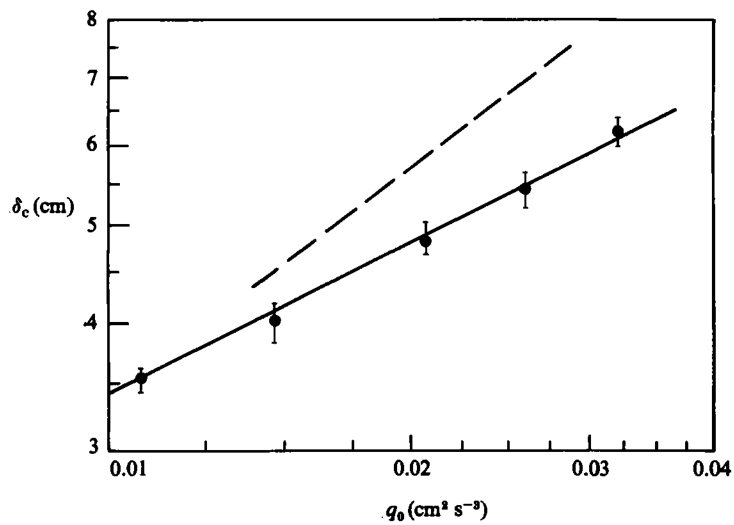

FIGURE 6. Variation of δ_c with q_0 at constant $N \approx 1.12\ s^{-1}$. The solid and broken lines correspond to $\frac{1}{2}$ and $\frac{3}{4}$ slopes respectively.

experiments with constant q_0 and variable N and vice versa, thereby checking what exponents for N and q_0 should be associated with the expression for δ_c. The results are depicted in figures 5–7 and show good agreement with (10). Using figure 7 it is possible to evaluate the average value for C_4 as $C_4 \approx 41.5$. Also noting that $C_4 = (C_1^2/C_2 C_3)^{\frac{3}{4}}$ with $C_1 \approx 1$ and $C_2 \approx 0.125$ (Fernando & Long 1985*a, b*) and $C_3 = (1/2 - C^{-2}) = 0.056$, we obtain $C_4 \approx 41.5$, which is in excellent agreement with the experimental results. However, it should be noted that the value of C_4 is extremely

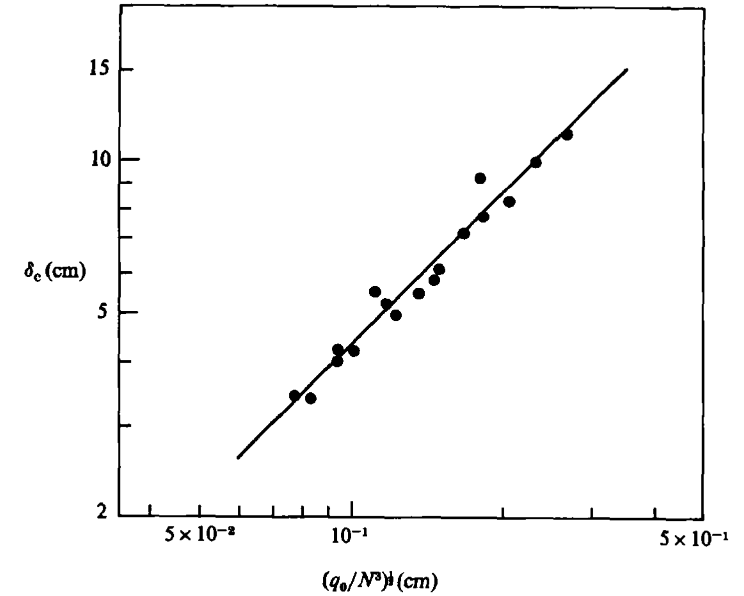

FIGURE 7. Variation of δ_c with $(q_0/N^3)^{\frac{1}{2}}$.

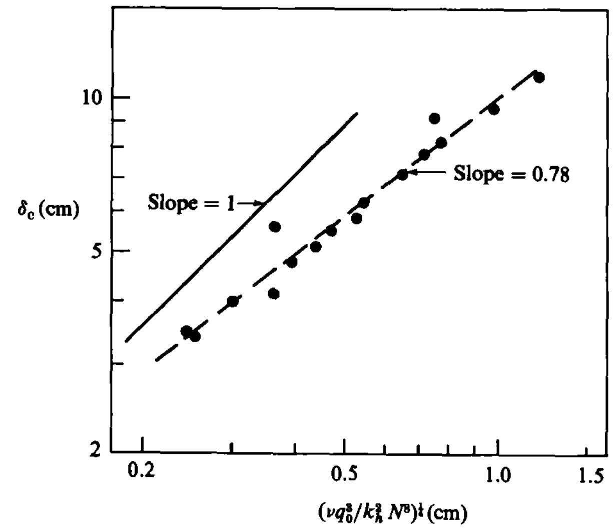

FIGURE 8. Variation of δ_c with $(\nu q_0^3/k_h^2 N^8)^{\frac{1}{4}}$. This plot is presented to compare the experimental results with (4). Note that although the data correlate well, the best slope is about 0.78 rather than 1 as given in (4).

sensitive to the choice of C, for which our measurements give an average value of 1.50.

In figure 8 we have plotted δ_c *vs.* $(\nu q_0^3/k_h^2 N^8)^{\frac{1}{4}}$ to compare the present results with the predictions of (4). Note that these results show that the best correlation would be $\delta_c \sim [(\nu q_0^3/k_h^2 N^8)^{\frac{1}{4}}]^{0.78}$, rather than what is expected on the basis of (4). It is interesting to note that the value of R_c calculated from our δ_c data (instead of the h_c data) yields an average of $R_c \approx 7.8\times10^4$, which is of the same order of magnitude as the value found by Turner (1968).

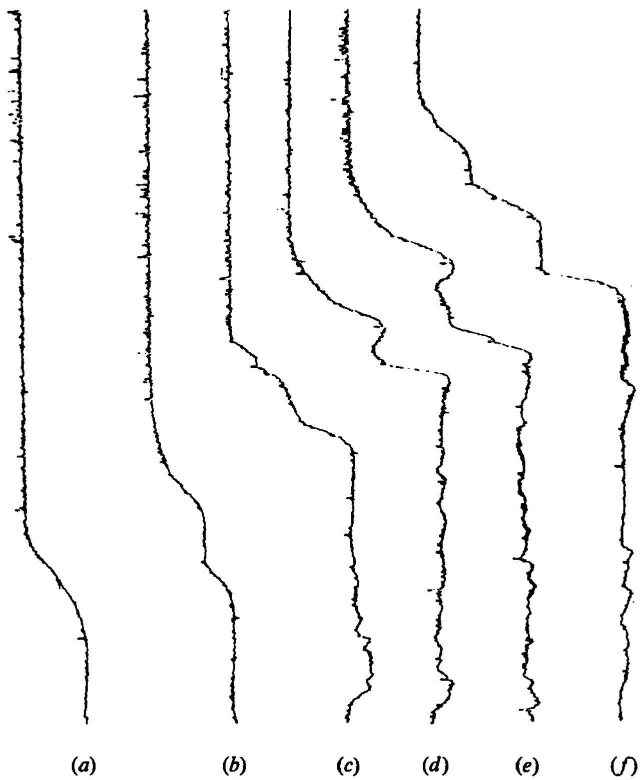

FIGURE 9. A sequence of temperature profiles obtained during the evolution of the layers. The vertical and horizontal axes represent the depth and the temperature. Profiles (a–f) correspond to the times $t = 130$, 180, 500, 700, 725 and 960 (in s) respectively.

4.4. *Measurement of temperature profiles*

Vertical temperature and salinity profiles were measured during various stages of the development of the mixed layer; figure 9 shows a sequence of such temperature profiles. Profile (a) was taken during the initial growth (at $t \approx 130$ s) and indicates the homogeneity of the mixed region and the presence of a thermal boundary layer above. As the mixed region grows further, the thermal boundary layer also seems to grow until it breaks down to form a second mixed region. Profile (b) was taken at $t \approx 180$ s, about 20 s after the appearance of the second mixed layer. Using the values pertaining to the experiment, $q_0 = 0.032$ cm^2/s and $N = 0.84$ s^{-1}, we may evaluate h_c using (4) as $h_c \approx 3.90$ cm, where $R_c \approx 10^3$, as suggested by Turner (1968), was used. This value is consistent with $h_c \approx 4.2$ cm obtained from profile (b). Profile (c), which was taken at $t \approx 500$ s, shows that the newly formed second layer has been entrained into the first layer, which is again topped by a thermal boundary layer. As the mixed layer grows further, the thermal boundary layer becomes unstable and forms another second mixed layer; this feature can be seen in profile (d), which was taken at $t \approx 700$ s.

It appears that there is a temperature inversion at the top of the second layer; this is probably due to the contact of the probe with eddies of the lower layer that protrude into the layer above distorting the interface. Field observations of Newman (1976) also show similar inversions when the mixed-layer thicknesses are small. Profile (e), which corresponds to $t \approx 725$ s, shows that the lower mixed layer has

Observation point	Observed (m)	Predicted using (4) with $R_c = 2.4\times10^4$	Predicted using (10) with $C_4 = 41.5$
A	1.20	2.00	1.87
B	0.55	0.40	0.60
C	1.40	1.40	1.42

TABLE 1. Comparison between the observed mixed-layer thicknesses of the thermohaline staircase structure of Lake Kivu (Newman 1976) and the theoretical predictions

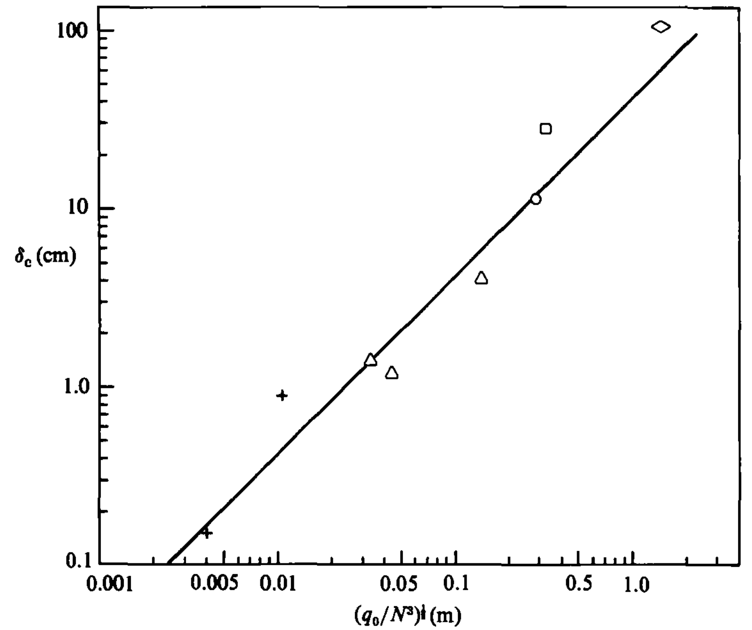

FIGURE 10. A plot of δ_c *vs.* $(q_0/N^3)^{\frac{1}{4}}$ from the geophysical data collected by Federov (1970): △, Lake Kivu (Newman 1976); +, Lake Vanda in Antarctica (Hoare 1966); □, Trenches in Red Sea (Swallow & Crease 1965); ◇, Mediterranean waters in Atlantic (Siedler 1968); ○, deep-water near-bottom geothermal inversions.

grown further, entraining the fluid from the layer above. Profile (*f*) was taken when the mixed layer had grown to δ_c, at which point the interface becomes quasi-stationary; the second layer can grow on it and the process continues to form a series of convecting layers separated by density interfaces. From profile (*f*), we may evaluate $\delta_c = 9.2$ cm, which is in agreement with that estimated using (10) as $\delta_c \approx 9.6$ cm. The measured electrical-conductivity profiles also showed similar behaviour, but owing to the temperature dependence of the conductivity, corrections need to be made before interpreting them quantitatively.

5. Discussion

We have discussed here some aspects of the layered structure that forms when a stable salinity gradient is subjected to heating from below. A simple theory was proposed to predict the critical height of the bottom layer at which a second convecting layer, separated by a quasi-stationary stable density interface, is formed. It was argued that this critical thickness of the bottom layer cannot be determined by a criterion based on the breakdown of the thermal boundary layer on the advancing turbulent front, owing to the possible entrainment of the newly formed layer into the lower layer. However, when the thickness of the lower layer grows to a certain size, which is determined by the balance of vertical kinetic and potential energies of the eddies, such entrainment cannot occur and two convecting layers separated by a quasi-stationary density interface can form. This process can continue to form a series of layers. However, the diffusive transfer of heat and salt across the interface causes the density difference between the layers to drop and, at a certain instant, eddies in the lower convecting layer can entrain fluid from the layer above. Then the interface tends to migrate slowly upwards until it merges with the next density interface. Occasionally during the migration, static instability may occur resulting in the merger of the layers. We have also presented a possible entrainment mechanism for the initial growth of the mixed layer.

The experiments corroborated the theoretical arguments and it was possible to evaluate certain constants appearing in the theory, which may be useful in interpreting some geophysical observations. For instance, Newman (1976) measured the thickness of the convecting layers observed in Lake Kivu, an East African rift lake, and compared the measurements with (4). As indicated in table 1, Newman's measurements were consistent with the h_c values calculated using (4) with $R_c = 2.4 \times 10^4$ (instead of $R_c \approx 10^3$), but the layer thicknesses predicted from the present formula (10), show a better agreement.

Federov (1970) has collected a set of field data on the step-like structure formed in the areas of oceans and lakes where the temperature and salinity increase with depth. In figure 10, we have plotted Federov's data, together with the predictions made using (10), Considering the possible sources of error due to differing laboratory and oceanic conditions, it is possible to conclude that there is a good agreement between the predictions and the field measurements.

During the period of this research, the author greatly benefitted from the encouragement and helpful comments of Professor D. F. Jankowski. Thanks are also due to Tom Nesdill, David McCormia and Paul Johnson for construction of the apparatus and running the experiments. The referees and Dr Dan Kelley of WHOI provided valuable comments that led to considerable improvements of the original version of this paper. This research was supported by National Science Foundation Grant No. MSM-8504909 and the Arizona State University Faculty Grant-in-Aid program.

REFERENCES

CARRUTHERS, D. J. & HUNT, J. C. R. 1986 Velocity fluctuations near an interface between a turbulent region and a stably stratified layer. *J. Fluid Mech.* **165**, 475–501.

CHEN, C. F., BRIGGS, D. G. & WIRTZ, R. A. 1971 Stability of thermal convection in a salinity gradient due to lateral heating. *Intl J. Heat & Mass Transfer* **14**, 57–65.

CRAPPER, P. F. & LINDEN, P. F. 1974 The structure of the turbulent density interfaces. *J. Fluid Mech.* **65**, 45–63.

CURRIE, I. G. 1967 The effect of heating rate on the stability of stationary fluids. *J. Fluid Mech.* **29**, 339–347.

DEARDORFF, J. W., WILLIS, G. E. & STOCKTON, B. H. 1980 Laboratory studies of the entrainment zone of a convective mixed layer. *J. Fluid Mech.* **100**, 41–64.

Federov, K. N. 1970 On the step-like structure of temperature inversions in the ocean. *Izv. Atmos. Ocean Phys.* **6**, 1178–1188.

Fernando, H. J. S. 1987*a* On the growth of a turbulent patch in a stratified fluid. *J. Fluid Mech.* (submitted).

Fernando, H. J. S. 1987*b* Buoyancy transfer across a diffusive interface separated by two convecting layers. *J. Fluid Mech.* (submitted).

Fernando, H. J. S. & Long, R. R. 1983 The growth of a grid-generated mixed layer in a two-fluid system. *J. Fluid Mech.* **133**, 377–395.

Fernando, H. J. S. & Long, R. R. 1985*a* On the nature of the entrainment interface of a two-layer fluid subjected to zero-mean-shear turbulence. *J. Fluid Mech.* **151**, 21–53.

Fernando, H. J. S. & Long, R. R. 1985*b* The deepening of a mixed layer in a linearly stratified fluid. *Phys. Fluids* **28**, 2999–3005.

Gregg, M. C. 1984 Persistent turbulent mixing and near-inertial waves. In *Internal Gravity Waves and Small Scale Turbulence* (ed. P. Muller & R. Pujalet), pp. 1–24. Hawaii Institute of Geophysics, Special Publication.

Hannoun, I. A., Fernando, H. J. S. & List, E. J. 1987 Turbulence structure near a sharp density interface. *J. Fluid Mech.* (in press).

Hoare, R. A. 1966 Problem of heat transfer in Lake Vanda, a density stratified arctic lake. *Nature* **210**, 787–789.

Howard, L. N. 1964 Convection at high Rayleigh numbers. In *Proc. 11th Intl Congress of Applied Mechanics, Munich* (ed. H. Görtler). Springer.

Hunt, J. C. R. 1984 Turbulence structure in thermal convection and shear-free boundary layers. *J. Fluid Mech.* **138**, 161–184.

Huppert, H. E. & Linden, P. F. 1979 On heating a stable salinity gradient from below. *J. Fluid Mech.* **95**, 431–464.

Incropera, F. P. & DeWitt, D. P. 1985 *Fundamentals of Heat and Mass Transfer.* Wiley.

Krause, G. 1968 Struktur und Verteilung des Wassers aus dem Roten Meer im Nordwesten des Indischen Ozeans. '*Meteor*' *Forschungsergebnisse* A, Heft 4.

Linbaugh, C. & Rechnitzer, A B. 1955 Visual detection of temperature–density discontinuities in water by dividing. *Science* **121**, 395.

Linden, P. F. 1973 The interaction of vortex rings with a sharp density interface: a model for turbulent entrainment. *J. Fluid Mech.* **60**, 467–480.

Linden, P. F. 1975 The deepening of a mixed layer in a linearly stratified fluid. *J. Fluid Mech.* **71**, 385–405.

Long, R. R. 1978 A theory of mixing in a stably stratified fluid. *J. Fluid Mech.* **84**, 113–124.

Lubimova, E. A., Richard, P., Von Herzen, R. P. & Udintzev, G. B. 1965 On heat transfer through the ocean floor. *Terrestrial Heat Flow.* Geophys. Monograph, vol. 8, p. 78.

Mack, S. 1985 Two-dimensional measurement of oceanic microstructure: the role of double diffusion. *J. Phys. Oceanogr.* **15**, 1581–1604.

Narimousa, S. & Fernando, H. J. S. 1987 On the sheared density interface of an entraining stratified fluid. *J. Fluid Mech.* **174**, 1–22.

Newman, F. C. 1976 Temperature steps in Lake Kivu: a bottom heated saline lake. *J. Phys. Oceanogr.* **6**, 157–163.

Oster, G. & Yamamoto, M. 1963 Density gradient techniques. *Chem. Rev.* **63**, 257.

Schmitt, R. W. 1981 Form of the temperature–salient relationship in the central water: evidence of double diffusive mixing. *J. Phys. Oceanogr.* **11**, 1015–1026.

Shirtcliffe, T. G. L. & Calhaem, I. M. 1968 Measurements of temperature and electrical conductivity in Lake Vanda, Victoria Land, Antarctica. *New Zealand. J. Geol. Geophys.* **11**, 976–981.

Siedler, G. 1968 Schichtungs- und Bewegungsverhältnisse am Südausgang des Roten Meeres. '*Meteor*' *Forschungsergebnisse* A, Heft 4.

Stegan, G. R., Hendricks, P. J. & Muench, R. D. 1985 Vertical mixing on the Bering Sea shelf. In *The Ocean Surface: Wave Breaking, Turbulent Mixing and Radio Probing* (ed. Y. Toba & H. Mitsuyasu), pp. 553–558. Reidel.

SWALLOW, J. C. & CREASE, J. 1965 Hot salty water at the bottom of the Red Sea. *Nature* **205**, 165–166.

THORPE, S. A. 1977 Turbulence and mixing in a Scottish loch. *Phil. Trans. R. Soc. Lond.* A **86**, 125–181.

TURNER, J. S. 1968 The behaviour of a salinity gradient heated from below. *J. Fluid Mech.* **33**, 183–200.

TURNER, J. S. & STOMMEL, H. 1964 A new case of convection in the presence of vertical salinity and temperature gradients. *Proc. Natl Acad. Sci.* **52**, 49–53.

VERONIS, G. 1965 On finite amplitude instability in thermohaline convection. *J. Mar. Res.* **23**, 1–17.

WOODS, J. D. 1968 Wave induced shear instability in the summer thermocline. *J. Fluid Mech.* **32**, 791–800.